Available online at https://doi.org/10.36303/SATNT.2021cosaami.44
Conference of the South African Advanced Materials Initiative

Effect of Nb glue atom in the cluster formula on the microstructure and mechanical properties of Ti-Mo alloy

L Raganya[a,b*], N Moshokoa[a, b], B Obadele[b,c], E Makhatha,[b] R Machaka[a,b]

[a]*Advanced Materials Engineering, Manufacturing Cluster, Council for Scientific and Industrial Research, Meiring Naudé Road, Brummeria, Pretoria 0184, South Africa*
[b]*Department of Metallurgy, University of Johannesburg, Doornfontein Campus, Johannesburg, South Africa*
[c]*Department of Chemical, Materials and Metallurgical Engineering, Botswana International University of Science and Technology, 10071 Boseja, Palapye, Botswana*
Email: address-leeragm@gmail.com

Abstract

The effect of Nb in the glue site of the cluster-plus-glue atom model formula on the microstructure and mechanical properties of Ti-Mo alloy was investigated. Phase and microstructural analysis were performed by X-ray diffraction and electron backscatter diffraction. Tensile properties were also examined. A small amount of secondary martensitic α" and ω_{ath} nano-particles were precipitated in the β matrix of both alloys, due to to the inhomogeneous distribution of Mo and/ or Nb caused by segregation, which formed local regions with high- and low-stability of the β phase. The elastic modulus was significantly reduced to 56.9 ± 3.08 GPa, while the elastic admissible strain was substantially improved. The increased β stability and suppression of the ω_{ath} phase led to no significant change in both the yield and ultimate tensile strengths, and the brittle fracture behavior. The alloy can be a potential alternative of the conventional orthopedic implant materials in orthopedic applications.

Keywords: Alloy design; β stability; segregation; metastable β-type Ti alloys

1. Introduction

The development of metastable β-type Ti alloys has recently been getting considerable attention as potential alternatives for the conventional orthopaedic materials which include cobalt-chromium (Co-Cr) based, 316L stainless steel (SS), CP Ti and Ti6Al4V.[1,2] These conventional materials have higher elastic moduli (110-220 GPa) than that of the human bone (10-30 GPa), which can cause stress shielding and eventually implant failure.[3-5] Moreover, allergic and toxic effects aluminium, vanadium, nickel, cobalt and chromium, which dissociate from the alloys in the human body, causing long-term health problems, have been reported.[5,6]

Metastable β-type Ti alloys contain non-toxic β stabilizing elements such as molybdenum (Mo), niobium (Nb), hafnium (Hf) and tantalum (Ta). In our previous work, an as-cast Ti-11.8Mo alloy designed using a cluster plus-glue-atom (CPGA) model was developed.[7] The model had the formula $[Mo(Ti_{14})]Ti_1$, which consisted of the cluster part [(center atom)-$(shell\ atoms)_{14}$] and the glue atom part, $(glue\ atoms)_x$. The position of elements in the formula was based on their interaction, which is characterized by their enthalpy of mixing (ΔH). Mo with negative ΔH (-4 kJ/mol) was placed in the cluster centre, Ti with a positive ΔH (2 kJ/mol in the glue site, and Ti with an ΔH of zero (Ti=0 kJ/mol) in cluster shell.[8] The microstructure of the alloy exhibited predominant β phase and the alloy showed low elastic modulus.

In this study, the Ti glue atom is substituted with one Nb glue atom (ΔH 2 kJ/mol) in the cluster formula. Toxic effects of the Nb glue atom on the microstructure and mechanical properties was investigated.

2. Materials and methods

2.1 Alloy design

The alloy was designed using the CPGA model with the formula $[(Mo)(Ti_{14})]Nb_1$ and the compositions in wt% are given in Table 1. Phases were predicted using d-electron theory, which exploits the relationship between β phase stability and elastic properties by theoretically determining the bond order (*Bo)* and the metal d-orbital energy level (*Md*) parameters.[9] *Bo* measures the covalent bond between Ti and an alloying element, while *Md* correlates with the electronegativity and the metallic radius of elements. Each element has a specific Bo value and a specific Md value for the BCC cluster. The $\overline{Md}$ and $\overline{Bo}$ values of the alloys were calculated using equations 1(a) and 1(b) and plotted on a phase stability map exhibited in Figure 1.

$$\overline{Md} = \sum_{i=i}^{n} X_i \,.\, (Md_i) \qquad \text{Equation (1a)}$$

$$\overline{Bo} = \sum_{i=i}^{n} X_i \,.\, (Bo_i) \qquad \text{Equation (1b)}$$

whereby, X_i is the atomic fraction of component *i* in the alloy, $(Md)_i$ and $(Bo)_i$ are the respective values for component *i*.[9,10] Ti-11.8Mo alloy located in the β+ω region indicates that the alloy would precipitate the ω phase in the β matrix. Meanwhile the Ti-11.1Mo-10.8Nb alloy is located along the β/β+ω boundary, suggesting that the alloy would form predominant β phase.

Table 1: Cluster formula, composition, $\overline{Bo}$ and $\overline{Md}$ of the designed alloys

Cluster Formula	Composition (*wt%*)	$\overline{Bo}$	$\overline{Md}$
$[Mo(Ti_{14})]T_i1$	Ti-11.8Mo	2.81	2.42
$[Mo(Ti_{14})]Nb_1$	Ti-11.1Mo-10.8Nb	2.83	2.42

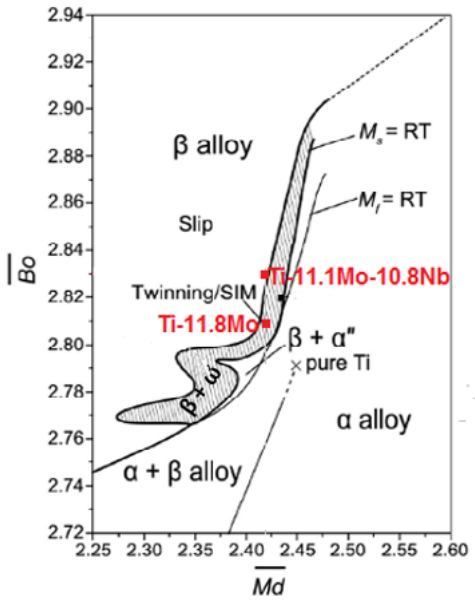

Figure 1: phase stability map[11]

2.2 Materials preparation and microstructural analysis

CP Ti (99.9%), Mo (99.5%) and Nb (99.8%) elemental powders were cold-compacted into 100 g green compacts, followed by melting in a water-cooled copper crucible with a tungsten electrode using a commercial arc remelting vacuum-pressure casting system. The melting chamber was evacuated and purged with argon before melting. The ingots were each flipped over and remelted three times to promote chemical homogeneity. Specimens for microstructural analysis were prepared using standard metallographic procedure and subsequently etched with Kroll's reagent containing 85 ml of distilled water, 15 ml of nitric acid and 5 ml of hydrofluoric acid. Phase constituents were identified using X-ray diffractometry (XRD) (XPERT-PRO diffractometer) equipped with Co Kα radiation and graphite monochrometer operated at 45 kV and 40 mA. The various Ti phases were identified by matching the observed XRD profile peaks with the Joint Committee on Powder Diffraction Standards files. EBSD analysis was conducted using the Oxford integrated Aztec HKL advanced EBSD system. Specimens were electro-polished in perichloric acid using a Struers polishing machine (LectroPol-5) at 30 V for 80 s.

2.3 Mechanical characterization

Tensile test specimens with 3 x 4 x 10 mm gauge dimensions were cut from the ingots via electrical discharge machining (EDM). Tensile tests were carried out at room temperature and the properties were measured using the Instron™ 1342 model apparatus.

3. Results and discussion

3.1 Phase and microstructural analysis

The XRD patterns of as-cast Ti-11.8Mo and Ti-11.1Mo-10.8Nb alloys with identified phases are presented in Figure 2. The BCC β phase diffraction peaks were detected in the XRD patterns in both alloys. Furthermore, diffraction peaks corresponding to the martensitic α" phase were also identified, indicating that the martensitic transformation start temperature was above room temperature. In both XRD patterns, small peaks at 2θ≈34° could also be distinguished and were identified as the ω_{ath} phase. The weak intensity of the ω phase peak could be attributed to its nano-size or small volume fraction. A similar ω peak was reported by Sadeghpour in ST Ti-Al-Mo-V-Cr alloy system.[12]

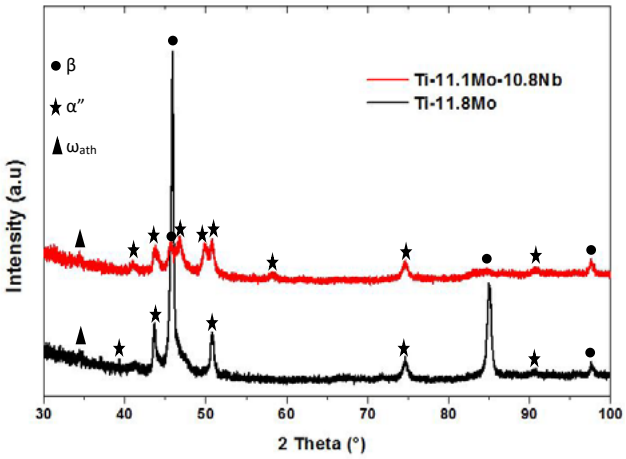

Figure 2: XRD patterns of Ti-11.8Mo and Ti-11.1Mo-10.8Nb alloys

The detailed microstructure was studied using EBSD analysis. The inverse pole figure (IPF) and phase maps of the alloys are depicted in Figure 3. The EBSD IPF maps of the Ti-11.8Mo and Ti-11.1Mo-10.8Nb alloys exhibited coarse, equiaxed *β* phase grains with nanoparticles embedded in the matrix and along the grain boundaries. The grain boundaries of the high temperature *β* phase could also be distinguished. The nano-particles precipitated in the β matrix were identified as secondary orthorhombic α" martensitic and the hexagonal ω_{ath} phases as shown in the phase maps. The phase maps exhibited a larger amount of the ω_{ath} phase in Ti-10.8Mo alloy than in the Ti-11.1Mo-10.8Nb alloy. This indicates that the substitution of the Ti glue atom with the Nb atom increased the stability of the β phase by suppressing the transformation of the β phase to ω_{ath} phase.

Depending on the concentration of the β stabilizers, metastable β-type Ti alloys can form different phases upon rapid cooling. Microalloying of Ti with low concentrations of the β stabilizing elements results in Ti alloys containing secondary precipitates in the β matrix (martensitic α"phase/ω_{ath} phase). When the concentration of the β stabilizing elements is sufficiently high, the precipitation of the secondary phases is suppressed, and the β phase is fully retained.[13] The microstructural findings showed that the Nb atom placed in the glue site increased the β stability, while suppressing the precipitation of the secondary α" and ω_{ath} phases. The observed secondary precipitates occurred due to the segregation of β stabilizing elements (both Mo and Nb) in the alloy

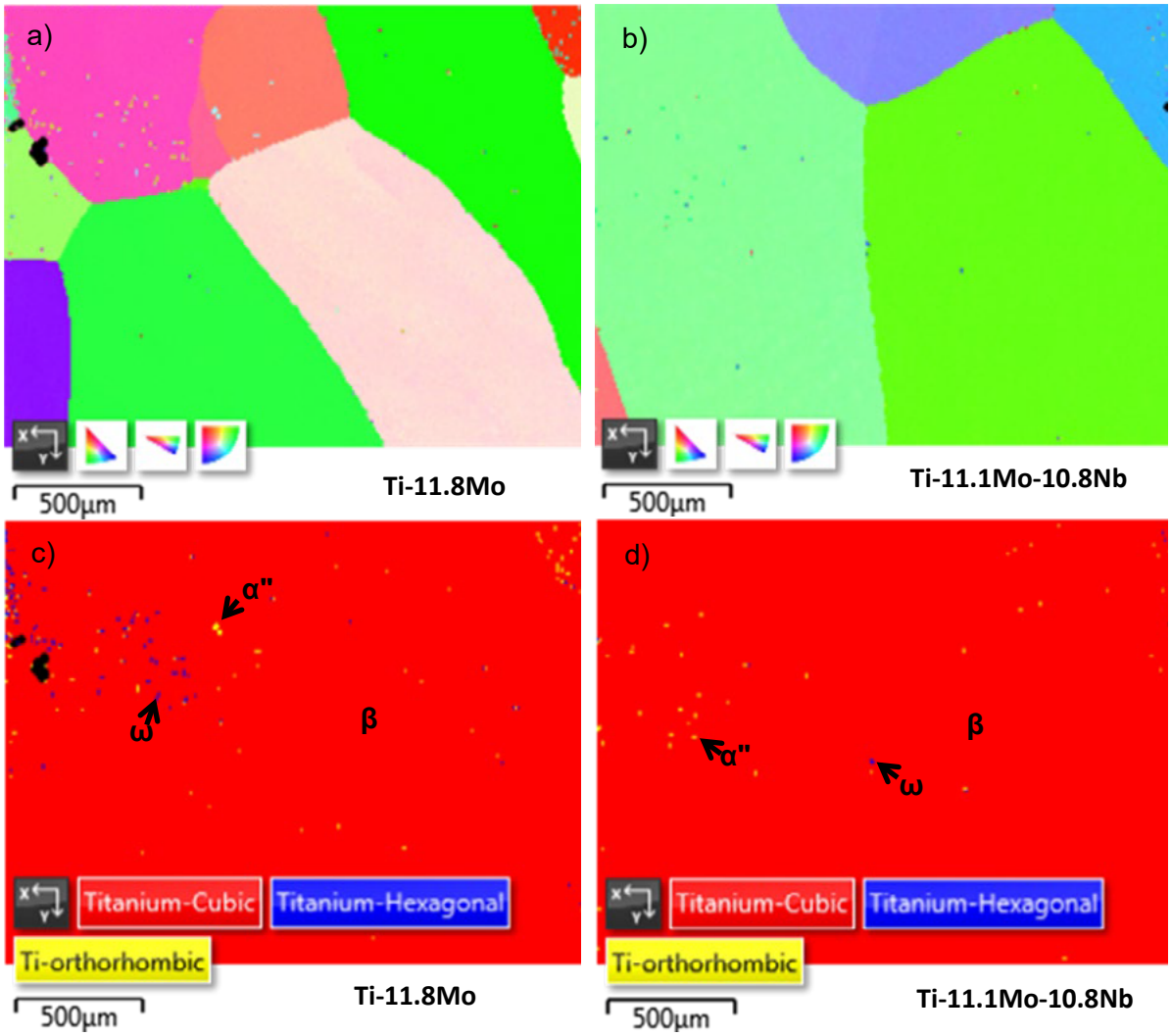

Figure 3: EBSD inverse pole figures (IPFs) of Ti-11.8Mo and Ti-11.1Mo-10.8Nb alloys

during solidification. This indicates that the distribution of both Mo and Nb in the alloy was not uniform, thus resulting in the formation of local regions rich- and lean in the β stabilizers. This led to the precipitation of the ω_{ath} and α" nano-particles preferentially in regions depleted in Mo and/ or Nb, while in the regions enriched with Mo and Nb, the transformation of the nano-particles was significantly hindered.

3.2 Mechanical properties

High tensile and yield strengths are a pre-requisite in the design of orthopaedic materials because they should sustain load-bearing function of human bones and reconstruction.[3] The tensile properties of the designed alloys and the conventional materials considered for comparison are listed in Table *2*, while the stress-strain curves are exhibited in Figure 4. It is evident that both the tensile and yield strengths of Ti-11.1Mo-10.8Nb alloy generally fell within the tensile and yield strengths range of 316L stainless steel and CoCrMo alloys. Meanwhile both strengths were lower than those of CP Ti. No significant change between the yield and ultimate tensile strengths of Ti-11.1Mo-10.8Nb and Ti-11.8Mo alloys was evident. This could be due to the suppression of the precipitation of the ω_{ath} phase in Ti-11.1Mo-10.8Nb alloy, which is known to induces precipitation hardening of the *β matrix.* Large elongation is desirable in orthopedic applications to prevent breakage incase an alloy is accidentally stressed beyond its proportional limit.[14] Although the elongation at fracture of the Ti-11.1Mo-10.8Nb alloy was higher than that of the Ti-11.8Mo alloy, both alloys failed in a brittle manner. The brittle fracture behavior of both alloys is also evident in Figure 4. The brittleness in the alloys could be partly attributed to the ω_{ath} nanoparticles which were clustered

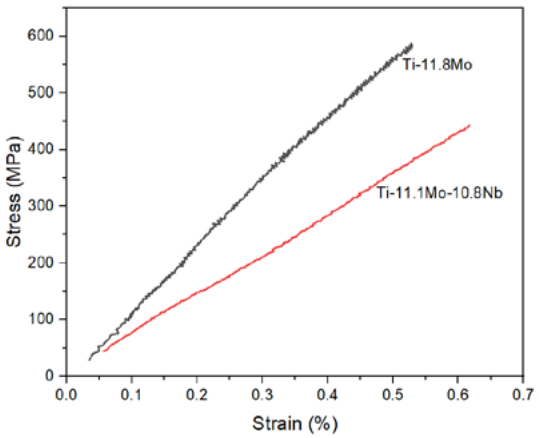

Figure 4: Tensile stress-strain curves of the investigated alloys

Table 2: Mechanical properties of the designed alloys and the conventional materials considered for comparison

Alloy	Yield Strength (MPa)	UTS (MPa)	Elongation (%)	Elastic modulus (GPa)	References
Bone	30–70	70–150	-	15-30	[20]
316 stainless steel	170–750	465–950	-	205–210	[20]
CoCrMo	275–1585	600–1785	-	210-253	[20]
CP Ti	692	785	-	105	[20]
Ti6Al4V	850- 900	960- 970	-	110	[20]
Ti-11.8Mo	639 ± 32.6	752 ± 28.3	0.52 ± 0.2	133.15 ± 10.52	This study
Ti-11.1Mo-10.8Nb	654 ± 47.1	671 ± 42.5	0.61 ± 0.3	56.9 ± 3.08	This study

considerably along the grain boundaries and within the grains, causing stress concentration. Similar brittle fracture behavior was reported in Ti-Ta-Zr-Nb [15] and Ti-Mo-Nb [16] alloy series. The combination of large elongation and high tensile strength results in good fracture resistance.[14] Therefore, the alloys in this study would have poor fracture resistance, due to their brittleness.

It is noteworthy that the elastic modulus of biomaterial must match that of the human bone (10 – 30 GPa) to prevent stress shielding effect during implantation. Ti-111.8Mo alloy showed high elastic modulus, which was similar to that of Ti6Al4V conventional alloy. The high elastic modulus was attributed to the large amount of the ω_{ath} phase precipitated in the alloy. Meanwhile, the elastic modulus of Ti-11.1Mo-10.8Nb alloy was substantially lower than the conventional materials' elastic moduli as shown in Table 2. It is evident that the substitution of the Ti glue atom with one Nb atom led to a significant reduction of the elastic modulus, due to the increased β phase stability. This elastic modulus value is substantially lower than the elastic moduli of Ti-Mo-Nb alloys reported in the literature.[17-19] Furthermore, Ti-11.1Mo-10.8Nb alloy possessed both lower elastic modulus and higher yield strength, which are also desirable for orthopaedic applications because of the large elastic recovery strain.

In orthopaedic applications, an ideal biomedical implant material is required to have greater elastic admissible strain. Elastic admissible strain is defined as the ratio of the strength over the elastic modulus of a material, and it is a useful parameter. The greater the elastic admissible strain, the more desirable the material is for such applications. Figure 5 displays the elastic admissible strains of the alloys and CP Ti, Ti6Al4V, Co-Cr and 316L stainless steel (SS) considered for comparison.[19] It is evident that the elastic admissible strain of the Ti-11.8Mo alloy was low compared to those of bone, CP Ti, Ti6Al4V and Co-Cr alloys, but higher than that of 316 L stainless steel. On the contrary, the substitution of the Ti glue atom with the Nb atom resulted in an elastic admissible strain far greater than those of the conventional alloys and the Ti-11.8Mo alloy. Therefore, the Ti-11.1Mo-10.8Nb alloy would offer promising performance in practical applications in terms of mechanical compatibility.

4. Conclusion

The effect of Nb glue atom on the microstructure and mechanical properties of Ti-Mo alloy designed using the cluster plus-glue-atom model was investigated. The observed microstructural and mechanical findings of the Ti-11.1Mo-10.8Nb alloy led to the following conclusions:

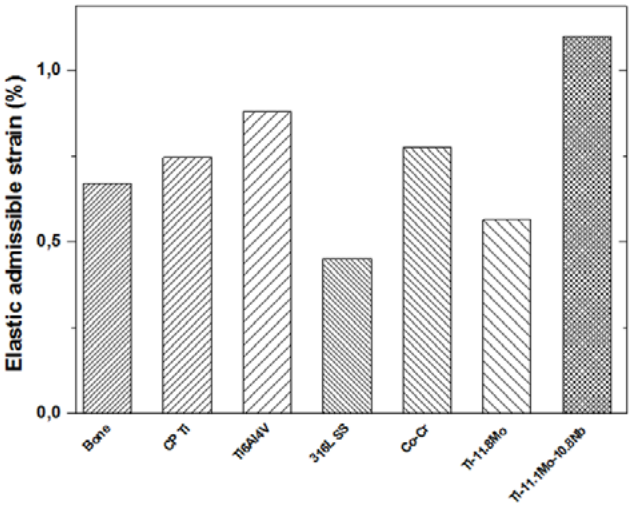

Figure 5: Elastic admissible strains of the designed alloys and the conventional materials are considered for comparison[21,22]

- The alloy consisted of predominant β phase, and a small fraction of the secondary phases caused by segregation of Mo and Nb during solidification.
- The elastic modulus was significantly reduced, while the elastic admissible strain was substantially improved.
- The increased β stability and suppression of the ω_{ath} phase led to no significant change in both the yield and ultimate tensile strengths. The ω_{ath} phase observed in the alloy caused brittle fracture.
- The alloy can be a potential alternative of the conventional orthopedic implant materials in orthopedic applications.

Acknowledgements

The authors would like to acknowledge the technical staff at Mintek, NIMSA and UP for their contribution.

Funding

This research was financially supported by the National Research Foundations (NRF), Council for Scientific and Industrial Research (CSIR) and the Department of Science and Innovation, South Africa, through Thuthuka Grant No. 115859.

Contribution of each author

Lerato Raganya: Conceptualization, Investigation, Methodology, Data curation, Writing - original draft, Writing - review & editing. **Nthabiseng Moshokoa**: Data curation, Investigation,

Methodology. **Babatunde Obadele, Elizabeth Makhatha & Ronald Machaka**: Supervision, Review & editing.

References

1. S. Guo, J. Zhang, X. Cheng, and X. Zhao, "A metastable β-type Ti–Nb binary alloy with low modulus and high strength," *J. Alloys Compd.*, vol. 644, pp. 411–415, 2015, doi: 10.1016/j.jallcom.2015.05.071.
2. R. Kolli and A. Devaraj, "A Review of Metastable Beta Titanium Alloys," *Metals (Basel).*, vol. 8, no. 7, p. 506, 2018, doi: 10.3390/met8070506.
3. K. S. Katti, "Biomaterials in total joint replacement," *Colloids Surfaces B Biointerfaces*, vol. 39, no. 3, pp. 133–142, 2004, doi: 10.1016/j.colsurfb.2003.12.002.
4. Y. Y. Li, C. Yang, H. Zhao, S. Qu, X. Li, and Y. Y. Li, "New developments of ti-based alloys for biomedical applications," *Materials (Basel).*, vol. 7, no. 3, pp. 1709–1800, 2014, doi: 10.3390/ma7031709.
5. M. B. Nasab, M. R. Hassan, and B. Bin Sahari, "Metallic biomaterials of knee and hip - A review," *Trends Biomater. Artif. Organs*, vol. 24, no. 2, pp. 69–82, 2010.
6. S. Guo, Q. Meng, X. Zhao, Q. Wei, and H. Xu, "Design and fabrication of a metastable β-type titanium alloy with ultralow elastic modulus and high strength," *Sci. Rep.*, vol. 5, no. September, pp. 1–8, 2015, doi: 10.1038/srep14688.
7. M. L. Raganya, N. M. Moshokoa, B. Obadele, P. A. Olubambi, and R. Machaka, "The microstructural and mechanical characterization of the β-type Ti-11.1Mo-10.8Nb alloy for biomedical applications," *IOP Conf. Ser. Mater. Sci. Eng.*, vol. 655, no. 1, p. 012025, Nov. 2019, doi: 10.1088/1757-899X/655/1/012025.
8. Q. Wang, C. Ji, Y. Wang, J. Qiang, and C. Dong, "β-Ti alloys with low young's moduli interpreted by cluster-plus-glue-atom model," *Metall. Mater. Trans. A Phys. Metall. Mater. Sci.*, vol. 44, no. 4, pp. 1872–1879, 2013, doi: 10.1007/s11661-012-1523-8.
9. M. Morinaga, "The molecular orbital approach and its application to biomedical titanium alloy design," in *Titanium in Medical and Dental Applications*, Elsevier, 2018, pp. 39–64.
10. M. Morinaga and H. Yukawa, "Alloy design with the aid of molecular orbital method," *Bull. Mater. Sci.*, vol. 20, no. 6, pp. 805–815, 1997, doi: 10.1007/BF02747420.
11. L. C. Zhang and L. Y. Chen, "A Review on Biomedical Titanium Alloys: Recent Progress and Prospect," *Adv. Eng. Mater.*, vol. 21, no. 4, pp. 1–29, 2019, doi: 10.1002/adem.201801215.
12. S. Sadeghpour, S. M. Abbasi, M. Morakabati, A. Kisko, L. P. Karjalainen, and D. A. Porter, "On the compressive deformation behavior of new beta titanium alloys designed by d-electron method," *J. Alloys Compd.*, 2018, doi: 10.1016/j.jallcom.2018.02.212.
13. S. Ehtemam-Haghighi, Y. Liu, G. Cao, and L. C. Zhang, "Phase transition, microstructural evolution and mechanical properties of Ti-Nb-Fe alloys induced by Fe addition," *Mater. Des.*, vol. 97, pp. 279–286, 2016, doi: 10.1016/j.matdes.2016.02.094.
14. W. F. Ho, T. Y. Chiang, S. C. Wu, and H. C. Hsu, "Mechanical properties and deformation behavior of cast binary Ti-Cr alloys," *J. Alloys Compd.*, vol. 468, no. 1–2, pp. 533–538, 2009, doi: 10.1016/j.jallcom.2008.01.046.
15. S. Ozan, J. Lin, Y. Li, and C. Wen, "New Ti-Ta-Zr-Nb alloys with ultrahigh strength for potential orthopedic implant applications," *J. Mech. Behav. Biomed. Mater.*, vol. 75, no. May, pp. 119–127, 2017, doi: 10.1016/j.jmbbm.2017.07.011.
16. L. J. Xu, Y. Y. Chen, Z. G. Liu, and F. T. Kong, "The microstructure and properties of Ti-Mo-Nb alloys for biomedical application," *J. Alloys Compd.*, vol. 453, no. 1–2, pp. 320–324, 2008, doi: 10.1016/j.jallcom.2006.11.144.
17. A. R. V. Nunes *et al.*, "Microstructure and Mechanical Properties of Ti-12Mo-8Nb Alloy Hot Swaged and Treated for Orthopedic Applications," *Mater. Res.*, vol. 20, no. suppl 2, pp. 526–531, 2017, doi: 10.1590/1980-5373-mr-2017-0637.
18. Q. Wang, X. D. Zhang, X. N. Li, C. J. Ji, and C. Dong, "Designing Multi-Component β-Ti Alloys with Low Young's Modulus," *Mater. Sci. Forum*, vol. 747–748, pp. 885–889, 2013, doi: 10.4028/www.scientific.net/MSF.747-748.885.
19. L. H. De Almeida, I. N. Bastos, I. D. Santos, A. J. B. Dutra, C. A. Nunes, and S. B. Gabriel, "Corrosion resistance of aged Ti – Mo – Nb alloys for biomedical applications," *J. Alloys Compd.*, vol. 615, pp. S666–S669, 2014, doi: 10.1016/j.jallcom.2014.01.173.
20. M. Navarro, A. Michiardi, O. Castaño, and J. A. Planell, "Biomaterials in orthopaedics," *J. R. Soc. Interface*, vol. 5, no. 27, pp. S. Ozan, J. Lin, Y. Li, R. Ipek, and C. Wen, "Development of Ti-Nb-Zr alloys with high elastic admissible strain for temporary orthopedic devices," *Acta Biomater.*, vol. 20, pp. 176–187, 2015, doi: 10.1016/j.actbio.2015.03.023.
21. Y. L. Zhou and D. M. Luo, "Microstructures and mechanical properties of Ti-Mo alloys cold-rolled and heat treated," *Mater. Charact.*, vol. 62, no. 10, pp. 931–937, 2011, doi: 10.1016/j.matchar.2011.07.010.